Journal of Applied Biomechanics, 2012, 28, 400-411

Journal of
APPLIED BIOMECHANICS
An Official Journal of ISB
www.JAB-Journal.com
ORIGINAL RESEARCH

Relationships Between Glide Efficiency and Swimmers' Size and Shape Characteristics

Roozbeh Naemi,[1] Stelios G. Psycharakis,[2,3] Carla McCabe,[2,3] Chris Connaboy,[2,3] and Ross H. Sanders[3]

[1]Staffordshire University; [2]Edinburgh Napier University; [3]University of Edinburgh

Glide efficiency, the ability of a body to minimize deceleration over the glide, can change with variations in the body's size and shape. The purpose of this study was to investigate the relationships between glide efficiency and the size and shape characteristics of swimmers. Eight male and eight female swimmers performed a series of horizontal glides at a depth of 70 cm below the surface. Glide efficiency parameters were calculated for velocities ranging from 1.4 to 1.6 m/s for female swimmers (and at the Reynolds number of 3.5 million) and from 1.6 to 1.8 m/s for male swimmers (and at the Reynolds number of 4.5 million). Several morphological indices were calculated to account for the shape characteristics, with the use of a photogrammetric method. Relationships between the variables of interest were explored with correlations, while repeated-measures ANOVA was used to assess within-group differences between different velocities for each gender group. Glide efficiency of swimmers increased when velocity decreased. Some morphological indices and postural angles showed a significant correlation with glide efficiency. The glide coefficient was significantly correlated to the chest to waist taper index for both gender groups. For the male group, the glide coefficient correlated significantly to the fineness ratio of upper body, the chest to hip cross-section. For the female group the glide coefficient had a significant correlation with the waist to hip taper index. The findings suggested that gliding efficiency was more dependent on shape characteristics and appropriate postural angles rather than being dependent on size characteristics.

Keywords: glide factor, glide coefficient, glide constant, anthropometry, morphological indices

Improving the glide performance in swimming starts and turns and the stroke cycle of breaststroke has been shown to positively affect the overall performance (Hay & Guimaraes, 1983; D'Acquisto et al., 1988). The glide performance is highly affected by the glide efficiency, which is defined as the ability of a body to minimize deceleration through the course of a glide. Naemi and Sanders (2008) showed that glide efficiency, which is influenced by the inertial and the resistive characteristics, is affected by the body's size and shape. These authors established that the glide factor, which is a product of a glide constant and a glide coefficient, is an indicator of glide efficiency. The glide constant incorporates the size-related parameters of the body, such as the body mass and the maximum cross-sectional area. The glide coefficient is related to the shape characteristics of the body while in a streamlined gliding position. The relationship between the glide parameters has previously been explored through the hydro-kinematic method (Naemi & Sanders, 2008):

$$C_G = \lambda \cdot C_g$$

where C_G represents glide factor, λ represents the glide constant in meters, and C_g is the dimensionless glide coefficient.

Figure 1, based on the findings of Naemi and Sanders (2008), presents a deterministic model that illustrates the relationship between the glide factor and the glide constant and coefficient. For the purposes of the current study, this model has been expanded to include the parameters that determine the size and shape characteristics affecting glide efficiency, as described in the following sections.

Several authors have examined the effect of size and shape parameters on the resistive characteristics. Size-related parameters, such as head and thorax circumference, depth and breadth, chest girth and maximum cross-sectional area, body surface area, mass and height, have been found to be positively correlated to the drag values (Clarys et al., 1974; Chatard et al., 1990; Lyttle et al., 1998; Benjanuvatra et al., 2001). Some shape-related

Roozbeh Naemi is with the Faculty of Health, Staffordshire University, Stoke-on-Trent, U.K. Stelios G. Psycharakis *(Corresponding Author)*, Carla McCabe, and Chris Connaboy are with the School of Life Sciences, Edinburgh Napier University, Edinburgh, U.K., and the Centre for Aquatics Research & Education, University of Edinburgh, Edinburgh, U.K. Ross H. Sanders is with the Centre for Aquatics Research & Education, University of Edinburgh, Edinburgh, U.K.

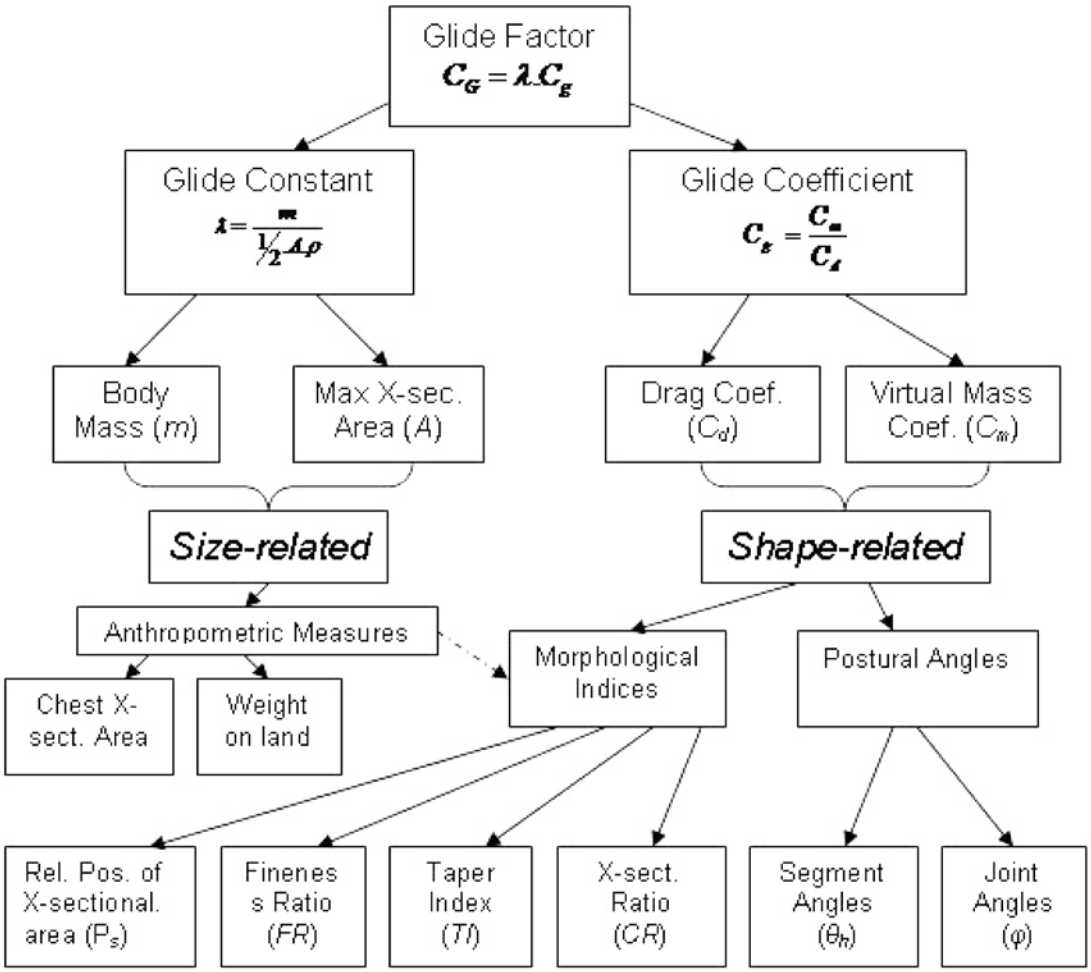

Figure 1 — The deterministic model of the glide factor and its contributing shape-related and size-related parameters. C_m: virtual mass coefficient (dimensionless), and C_d: drag coefficient (dimensionless).

parameters, such as the ratio of height to the maximum cross-sectional area, have been found to be negatively correlated to the resistive characteristics of the human body (Clarys et al. 1974; Clarys, 1978, 1979). As the glide coefficient depends on the shape of the body in a streamlined position, morphological indices from naval architecture and from the hydrodynamic studies of aquatic animals can be adapted to quantify the shape characteristics of the body (Clarys, et al., 1974). It should be noted that the shape of the body changes with variations in the body posture. For example, head position has been found to play an important role in the amount of resistance encountered by a swimmer (Miyashita & Tsunoda, 1978). In addition, the correlation between joint laxity and drag force indicates the ability of subjects with higher flexibilities to adopt a superior streamlining position that creates less resistance (Chatard et al., 1990). This suggests that the joint angles need to be considered as a determining factor for the drag forces.

Since the glide efficiency is influenced by both the resistive force and virtual mass, the latter being the sum of body mass and the added mass of water entrained with body (Naemi & Sanders, 2008), the relationship between these parameters and the size and shape characteristics needs to be established. An adapted version of the parameters and morphological indices that are generically used in the hydrodynamic study of aquatic animals is used here, to ensure that these parameters can identify the merits of the unique shape characteristics of the human body in a streamlined position.

For a body gliding underwater at a depth adequate to avoid wave drag, the glide efficiency (Figure 1) is affected by the same phenomena as the boundary layer and the flow separation, and may be determined by the boundary layer thickness and the size of the wake (Naemi & Sanders, 2008; Naemi et al., 2010). The body contours affect how the water flows over the body; it influences the thickness of the boundary layer at different parts of the body. Further, the areas of flow separation that determine the size of the wake are influenced by the body contours. To represent variations in body contour, relative changes in the cross-sectional area at various locations throughout the body can be

considered. These can be quantified as the morphological indices while the orientation of each cross-section relative to the flow can be quantified as the postural angles (Figure 1). The positions of each cross-section are important, as they determine the potential places where the flow would be separated from the body (Aleyev, 1977). Chest and buttocks are likely locations where flow separation may occur because of the abrupt changes in the flow direction. However, this has not been investigated yet.

An optimal ratio of body length to maximum diameter, known as fineness ratio of 4.5, has been assumed to decrease the drag forces (Hertel, 1966). As this is based on the investigation of the aquatic animals with almost circular cross-sectional areas (Fish & Hui, 1991), it would be interesting to calculate the fineness ratio during a glide for the human body, which has elliptical rather than circular cross-sections (Wicke & Lopers, 2003). Fineness ratio is a parameter commonly defined for streamlined objects that have a gradual increase in the cross-sectional area from tip to the midbody followed by a gradual decrease or tapering to the body end. Unlike the common streamlined objects, the swimmer's body (Figure 2) has a gradual increase in the cross-sectional area from finger tips to chest and a gradual decrease from there to waist, followed by another increase in the cross-sectional area from waist to buttocks and a gradual decrease afterward down to the to the toes. Thus the swimmer's body can be assimilated into two streamlined fuselages trailing along each other.

In addition to the above, there is a need for defining the parameters that quantify the changes in the cross-sectional ratios, to reflect how the flow changes as it moves from one cross-section of the body to another. To achieve this, modified version of the parameters and morphological indices that are generically used in the hydrodynamic study of aquatic animals is used here.

The purpose of the current study was to investigate the relationships between size and shape characteristics and glide efficiency of male and female swimmers for a range of gliding velocities, to further examine the efficacy of the glide factor.

Methods

Participants

Sixteen swimmers (eight male and eight female) competing at regional, national and international level participated in this study. Ethical approval was granted by the university ethics committee and all swimmers signed informed consent forms. The descriptive data for the swimmers are shown in Table 1.

Data Collection

The procedure and protocol for glide efficiency measurements was adopted from Naemi and Sanders (2008). In brief, swimmers pushed off from the wall at a depth of 70 cm below the surface and adopted a streamlined position (arms extended forward toward the direction of travel; hands pronated and overlapping; feet together and plantar flexed). A JVC KY-F32 camera (50 Hz) was positioned underwater, 10 m away from the swimmers, with its axis perpendicular to the glide path. A second camera was mounted at a 5 m height directly above the swimmers with its axis perpendicular to the intended glide path. The overhead camera was used for quality control, to ensure that swimmers did not deviate from the pool T-line. Swimmers were requested to sustain a horizontally aligned position and to maintain the depth during the glide. The glide intervals were selected from the acceptable glide sequences of each trial that complied with the condition of no deviation from the pool T-line or horizontal alignment. A minimum of 20 acceptable glide intervals for each individual were used for the analysis.

Selection and Calculation of Anthropometric Variables

Anthropometric variables were measured for the swimmers on land in an upright position, simulating as closely as possible the streamlined position adopted during the underwater glide. A photogrammetric method was used to determine the anthropometric measurements. The procedure and anatomical landmarks used have been described by Naemi and Sanders (2008).

The body was divided in the upper zone (from the waist level to dactylion) and the lower zone (from the akropodion level to the waist level), and five measurement levels were defined (Table 2). Based on combing the fluid dynamic principles reviewed extensively in Naemi et al. (2010) with the results of previous computational fluid dynamics (CFD) studies of the flow around the swimmer (e.g., Bixler et al., 2007) that allowed flow visualization, the potential locations at which the flow separation occurs were predicted. Moreover, a pilot study was conducted to qualitatively assess the potential areas of flow separation using tufted full-body suit. A swimmer wearing a tuft suit was filmed during a glide, to identify the potential locations of flow separation. As the direction of tufts can show the flow direction close to the body during a glide, wobbling tufts show a separated flow and straight tufts show an attached flow. Thicknesses and breadths of the areas of interest at each measurement level were calculated from the digitized outline (Figure 2). The cross-sectional areas were calculated based on the assumption that the segmental cross-sectional area of a human body could be well modeled by an appropriate ellipse with the same thickness and breadth (Jensen, 1978; Wicke & Lopers, 2003). Ten heights or vertical distances of interest were calculated as described in Table 3.

The area of each cross-section was calculated at each level with the following equation

$$A_c = \frac{\pi}{4} \times B \times T$$

where A_c represents the cross-sectional area, B is the breadth and T represents the thickness of the corresponding cross-sectional area.

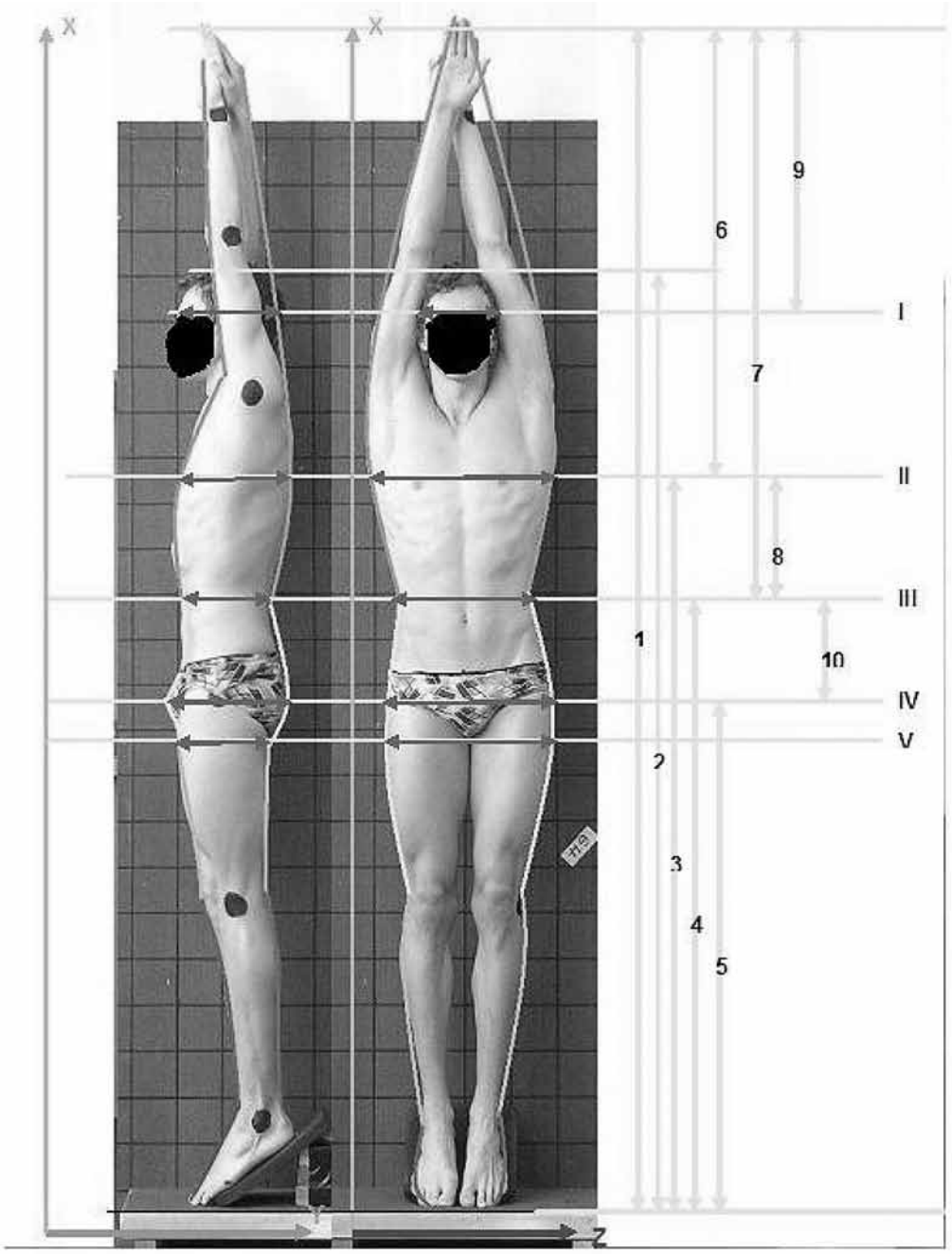

Figure 2 — Sample photographs of a swimmer, taken from front and side views. The five measurement levels (I to IV; see also Table 2) and nine heights (1–9; see also Table 3) calculated in this study are also shown. X: The longitudinal axis perpendicular to the transverse plane; Y: The frontal axis perpendicular to the frontal plane; Z: The sagittal axis perpendicular to the sagittal plane.

Selection and Calculation of Morphological Indices

The body was considered as two zones attached at the waist, so that each part has a gradual increase in the cross-sectional area followed by a gradual decrease. In the case of the upper zone, the cross-sectional area increases from the dactylion to the chest area and from there decreases to the waist. For the lower zone the cross-sectional area increases from the waist to the hip level and then decreases down to the akropodion. By dividing the body into these two zones it became possible to define a more specific hydrodynamic characteristic for each zone. This allowed the fineness ratio to be defined for each zone as well as for the whole body. The following morphological indices were used to quantify the body contour: the

Table 1 The mean ± *SD* for age, height, mass, and training volume for the swimmers in the present study

Group	Age (years)	Height (cm)	Mass (kg)	Distance/week (km)
Female ($N = 8$)	22.3 ± 2.2	173.5 ± 7.7	66.8 ± 5.2	24.3 ± 7.4
Male ($N = 8$)	19.4 ± 3.0	186.2 ± 5.9	77.5 ± 4.9	44.5 ± 6.2

Table 2 The five measurement levels defined for this study (see also Figure 2)

Measurement Levels		Locations
I	Forehead	Horizontal level immediately superior to glabella (portions of the frontal bone between the supraorbital ridges)
II	Chest	At the level of mesosternale
III	Waist	At the level of minimum girth around the waist
IV	Hip	At the level of the greatest posterior protuberance of the buttocks
V	Thigh	At a level 2 cm below the gluteal fold

Table 3 The 10 heights or distances of interest measured in this study (see also Figure 2)

Height/Distance		Vertical Distance Used for the Calculation
1	Streamlined height	Between the akropodion (the most superior point of the foot that may be the first or second digit) and dactylion (the most distal point of the third digit of the hand)
2	Head height	Between the akropodion (ground level) and vertex (the most superior point on the skull) of the head
3	Chest height	Between the akropodion (ground level) and the chest level
4	Waist height	Between the akropodion (ground level) and the waist level
5	Hip height	Between the akropodion (ground level) and the hip level
6	Chest to dactylion distance	Between the chest level and dactylion (top level)
7	Waist to dactylion distance	Between the waist level and dactylion (top level)
8	Waist to chest distance	Between the waist level and the chest level
9	Head to dactylion distance	Between the head level and dactylion (top level)
10	Hip to waist distance	Between the hip level and the waist level

relative position of maximum cross-sectional area, the fineness ratio, the taper index and the cross-sectional ratio. These were based on the fluid dynamics principles and on how the flow moves around the swimmer, as discussed by Naemi et al. (2010).

The relative position of each cross-section with regards to each zone's length or the whole body length was defined as

$$P_s = \frac{h_c}{h_z}$$

where h_c represents the vertical distance between each level and the superior level for each zone (in meters), h_z represents the height of each zone or the total height of body in the streamlined position (meters) and P_s represents the relative position of cross-section (dimensionless).

For the calculation of the fineness ratio, a nominal diameter was defined for each cross-section representing the diameter of the circle that has the same area as the cross-sectional area of the ellipse that approximates the cross-section of body

$$d_{nom} = \sqrt{\frac{4 \cdot A_c}{\pi}}$$

where d_{nom} represents nominal diameter (meters) and A_c represents the cross-sectional area (square meters).

The nominal diameters of cross-sectional areas at chest and hip were calculated as representing the maximum cross-sectional areas of the upper and lower zones. The fineness ratio was defined as

$$FR = \frac{h_z}{d_{nom}}$$

where h_z represents the height of each zone or the total height of body in the streamlined position (m), d_{nom} represents nominal diameter (m) and FR is the dimensionless fineness ratio.

A taper index can be defined to account for the magnitude of the direction changes as the particles in the flow pass from one cross-sectional area to another. Since the areas behind the buttocks and back are vulnerable to flow separation, the taper indices from the chest to waist, waist to hip and hip to thigh are useful in quantifying the potential for flow separation in these areas. Although flow separation can only be quantified with flow visualization techniques like CFD, a lower glide efficiency may indicate flow separation. A taper index was defined as the ratio of changes in the cross-sectional area to the distance between the two consequent cross-sections:

$$TI = \frac{A_{c1} - A_{c2}}{x_{c1} - x_{c2}}$$

where TI represents taper index in meters, A_c represents the cross-sectional area in square meters and x_{c1} represents the vertical coordinate of the corresponding cross-section in meters.

The ratio of two cross-sectional areas was calculated as

$$CR = \frac{A_{c1}}{A_{c2}}$$

where CR represents the cross-sectional ratio and A_c represents the area corresponding to the cross-section.

Selection and Calculation of Postural Angles

Segmental angles were calculated based on the joint center's coordinates during glide intervals as follows:

$$\theta_h = \frac{180}{\pi} \times \arctan \frac{y_s - y_i}{x_s - x_i}$$

where θ_h is the segmental angle of attack (degrees), y represents joint's vertical coordinate during the glide and x represents joint's horizontal coordinate. The term S corresponds to the superior and i to inferior joints.

Seven segments were considered: hand, arm (forearm and upper arm together), trunk, thigh, shank, foot and head. As the elbow's axis of rotation was not parallel to the optical axis of the camera, the forearm and upper arm were considered together. The segmental angles of the adjacent segments were used to calculate the joint angles as shown below. Six joint angles including wrist, shoulder, neck, hip, knee and ankle were calculated (Figure 3) as follows:

$$\varphi = \theta_n - \theta_{n-1}$$

where θ_i is the segmental angle of attack for an inclined rectilinear glide (degrees) and φ is the joint angle (degrees).

Calculation of Glide Efficiency Parameters

The glide factor was calculated based on the curve fitting technique (Naemi & Sanders, 2008). Glide constant was calculated according to the following formula:

$$\lambda = \frac{m}{\frac{1}{2} \cdot A \cdot \rho}$$

where λ represents the glide constant, m represents body mass in kilograms, A represents maximum cross-sectional area (chest cross-sectional area) in square meters and ρ represents the water density (kg/m^3).

The glide coefficient was calculated as

$$C_g = \frac{C_G}{\lambda}$$

Because of the differences in the attainable glide velocities between the gender groups, the glide efficiency parameters were calculated at the velocities of 1.4, 1.5 and 1.6 m/s for the female group and at the velocities of 1.6, 1.7 and 1.8 m/s for the male group. Moreover, as the glide efficiency parameters change with the Reynolds number, these parameters were calculated for identical Reynolds numbers across swimmers. Because of the differences in the streamlined length between the gender groups, the glide coefficients were calculated at a Reynolds number of 3.5 million for the female group and at a Reynolds number of 4.5 million for the male group. Since the glide coefficient is a dimensionless parameter, it needs to be measured relative to dimensionless velocity (Reynolds

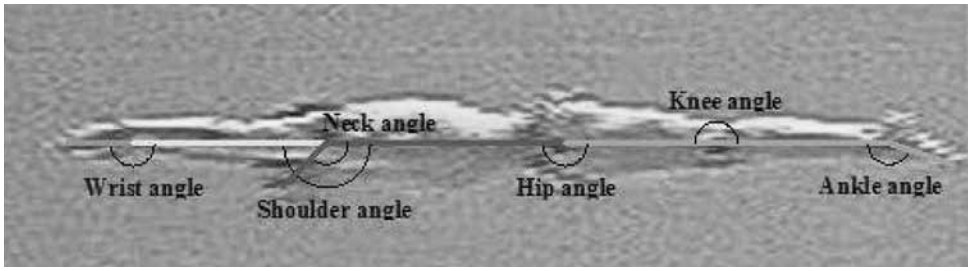

Figure 3 — The joint angles of a swimmer while gliding in a horizontal position.

number). The Reynolds number was calculated based on the average velocity during the glide and knowing the length (streamlined height) of the swimmer. For further information on the methods of calculating Reynolds number from the range of average velocities during the glide, readers are encouraged to consult Naemi and Sanders (2008). The calculated Reynolds numbers correspond to the velocities of 1.6 m/s and 1.8 m/s for the female and the male groups receptively.

During the initial assessment, most of the anthropometric measures and morphological indices were found to be significantly different between the male and female groups. This was also the case when the joint and segmental angles were compared between the two gender groups. Given the above, as well as the differences in the Reynolds number, it was decided to separate the gender groups for the subsequent statistical analyses.

Statistical Analysis

The SPSS software (version 14, SPSS Inc, USA) was used for statistical analysis. Given that differences in the glide coefficient and the glide factor have not been assessed for the velocities tested in the current study and that these variables were calculated for different velocity ranges for each gender group, a repeated-measures ANOVA was performed for each gender group to examine the within-group differences. Mauchly's test was used to assess sphericity and the Greenhouse–Geisser adjustment was applied when sphericity was violated. When significant differences were found, post hoc comparisons were conducted for all pairs of different velocities and a Bonferroni adjustment was applied to reduce the alpha level and eliminate the possibility of type I errors. Moreover, an independent *t* test was used to examine any between group differences for the common testing velocity of 1.6 m/s. The Pearson product–moment correlation coefficients were calculated between the glide coefficient and all morphological indices at the Reynolds number of 4.5 million for the male and 3.5 million for the female group, respectively. For all statistical analyses, significance was accepted at $p < .05$.

Results

The glide constant was 1.80 ± 0.14 m for the female group and 1.88 ± 0.08 m for the male group. The glide factor and glide coefficient at each velocity are presented in Table 4. The glide factor and glide coefficient decreased significantly when velocity increased in both groups. All pairwise comparisons for the glide factor and glide coefficient were statistically significant ($p < .001$) for the female group. For the male group, all pairwise comparisons for the glide coefficient were statistically significant ($0.014 \le p \le .015$). The glide factor for the male group was significantly lower at 1.8 m/s than at 1.6 m/s ($p = .033$), but not significantly different for any other pairwise comparisons. When calculated according to the Reynolds numbers, the glide coefficient was 2.59 ± 0.54 for the female group (at Reynolds number of 3.5 million) and 2.47 ± 0.61 for the male group (at Reynolds number of 4.5 million). For the common testing velocity of 1.6 m/s, there were no between-group differences in the glide factor ($p = .39$) or glide coefficient ($p = .19$).

The data for the position of maximum cross-sectional area, fineness ratio, tapering indices and cross-sectional ratios are presented in Table 5. Table 6 shows the correlations between the glide coefficient and the shape characteristics. Finally, the data for segmental and joint angles are shown in Table 7. The glide coefficient had a positive significant correlation with the chest to waist taper index for both groups. There were also positive significant correlations between the glide coefficient and ratio of chest to hip cross-sectional areas (for the male group only), and the waist to hip taper index (for the female group only). Finally, the glide coefficient for the male group had a negative significant correlation with the fineness ratio of the upper body, the hip angle and the knee angle.

Discussion

The results of this study indicated that both the glide factor and glide coefficient decreased significantly when velocity increased. This emphasizes the importance of the separate calculation of the glide efficiency parameters for

Table 4 The mean ± *SD* values for the glide factor calculated for the male and female groups at corresponding velocities

Females				
Velocity (m/s)	1.4	1.5	1.6	Repeated-Measures ANOVA
Glide factor (m)	4.93 ± 0.70	4.59 ± 0.70	4.25 ± 0.69	$F = 346.3$ ($p < 0.001$)*
Glide coefficient	2.77 ± 0.53	2.58 ± 0.51	2.39 ± 0.50	$F = 224.8$ ($p < 0.001$)*
Males				
Velocity (m/s)	1.6	1.7	1.8	Repeated-Measures ANOVA
Glide factor (m)	4.98 ± 1.30	4.73 ± 1.12	4.49 ± 0.95	$F = 8.8$ ($p = 0.003$)*
Glide coefficient	2.66 ± 0.73	2.53 ± 0.62	2.40 ± 0.52	$F = 14.7$ ($p = 0.005$)*

* Significant at $p < 0.05$.

Table 5 The average and standard deviation of the position of maximum cross-sectional area, fineness ratio, tapering indices and cross-sectional ratios for male, female and the pooled group

	Female		Male		Pooled	
Morphological Indices	**Avg.**	***SD***	**Avg.**	***SD***	**Avg.**	***SD***
Position of head to whole body	0.2	0.02	0.22	0.03	0.21	0.03
Position of chest to whole body	0.38	0.01	0.37	0.01	0.38	0.01
Position of waist to whole body	0.48	0.01	0.49	0.02	0.49	0.02
Position of chest to upper body	0.8	0.02	0.75	0.04	0.78	0.04
Position of hip to lower body	0.15	0.02	0.16	0.03	0.15	0.02
Fineness ratio of whole body	9.83	1.99	10.1	2.34	9.97	2.12
Fineness ratio of upper body	4.68	0.84	4.99	0.96	4.83	0.78
Fineness ratio of lower body	3.37	0.69	3.08	0.14	3.23	0.50
Hip to thigh taper index (m)	0.05	0.04	0.12	0.07	0.08	0.07
Chest to waist taper index (m)	0.13	0.04	0.12	0.04	0.13	0.04
Waist to hip taper index (m)	–0.13	0.04	–0.13	0.02	–0.14	0.03
Chest to hip cross-section	1.05	0.13	1.07	0.09	1.06	0.11
Hip to waist cross-section	1.62	0.14	1.69	0.16	1.65	0.15
Chest to waist cross-section	1.7	0.25	1.79	0.16	1.75	0.21

Table 6 The correlations between the glide coefficient and the shape characteristics

	Female (at Reynolds 3.5 million)		Male (at Reynolds 4.5 million)	
Shape Characteristic	***R***	***p***	***r***	***p***
Position of head to whole body	–0.516	0.191	–0.273	0.513
Position of chest to whole body	–0.112	0.792	0.346	0.401
Position of waist to whole body	–0.247	0.555	-0.550	0.158
Position of chest to upper body	0.025	0.953	0.542	0.165
Position of hip to lower body	0.399	0.168	0.117	0.391
Fineness ratio of whole body	–0.480	0.229	–0.527	0.180
Fineness ratio of upper body	–0.492	0.216	–0.788*	0.020*
Fineness ratio of lower body	–0.577	0.134	–0.390	0.340
Hip to thigh taper index (m)	0.220	0.601	0.432	0.285
Chest to waist taper index (m)	0.732*	0.039*	0.808*	0.015*
Waist to hip taper index (m)	0.718*	0.045*	–0.515	0.192
Chest to hip cross-section	0.550	0.158	0.759*	0.029*
Hip to waist cross-section	0.364	0.375	–0.234	0.577
Chest to waist cross-section	0.680	0.064	0.577	0.134
Hand segment	0.254	0.544	–0.179	0.672
Wrist angle	0.671	0.069	0.064	0.880

(continued)

Table 6 *(continued)*

	Female (at Reynolds 3.5 million)		Male (at Reynolds 4.5 million)	
Shape Characteristic	***R***	***p***	***r***	***p***
Arm segment	–0.359	0.383	–0.203	0.630
Shoulder angle	0.396	0.332	0.353	0.391
Head segment	–0.228	0.587	–0.225	0.592
Neck angle	0.263	0.529	0.363	0.377
Trunk segment	0.323	0.435	0.578	0.133
Hip angle	–0.086	0.840	–0.88*	0.040*
Thigh segment	0.415	0.307	–0.704	0.051
Knee angle	0.600	0.116	–0.709*	0.049*
Shank segment	–0.339	0.411	0.611	0.108
Ankle angle	–0.273	0.513	–0.09	0.832
Foot segment	–0.667	0.071	0.626	0.097

*Significant at $p < 0.05$.

Table 7 The average and standard deviation for different segmental and joint angles for male, female and the pooled group for horizontal glides

Segment/Joint	Female		Male		Pooled	
Angle (degrees)	**Avg.**	***SD***	**Avg.**	***SD***	**Avg.**	***SD***
Hand	1	7	–2	4	–1	5
Wrist	170	5	177	5	173	6
Arm	11	4	1	5	6	6
Shoulder	163	7	176	7	169	9
Head	53	14	39	9	46	14
Neck	121	17	138	10	129	16
Trunk	–7	3	–3	3	–5	3
Hip	189	5	186	3	188	4
Thigh	3	2	3	2	3	2
Knee	182	3	181	5	181	4
Shank	1	2	3	4	2	3
Ankle	168	3	166	4	167	4
Foot	–11	2	–11	3	–11	3

different swimming velocities. This is a consequence of the glide coefficient being dependent on how the flow moves around the swimmer, which, in addition to the body shape, is dependent on the flow characteristics that change at different gliding velocities.

The relationship between the size and the shape characteristics of a body in a streamlined position and its glide efficiency and hydrodynamic parameters had not been determined previously. The main aim of this study was to investigate the relationship between the glide efficiency parameters and the size and the shape characteristics quantified by the anthropometric measures, morphological indices and postural angles of a body in a streamlined position. Although the existence of a significant correlation does not necessarily imply a cause and effect between two parameters, it enables us to

identify the size and shape characteristics of bodies with superior hydrodynamic gliding efficiency.

The results indicated that the shape-related glide efficiency parameters were associated more with glide efficiency than were the size-related parameters. It can be stated that swimmers with superior shape (determined by a higher glide coefficient) tend to glide more efficiently than swimmers with a superior size (determined by a higher glide constant). These findings emphasize the relative importance of the shape-related parameters compared with the size-related parameters when considering the efficiency of the glide. While mathematically increasing the glide constant or the glide coefficient would increase the glide factor, the findings suggested that the disadvantage of having a nonoptimum size may be compensated by an appropriate shape. This may explain how some of the best swimmers in the current study with large chest cross-sectional areas, which would be expected to create a high resistive force, performed better than swimmers with smaller cross-sectional areas.

It is also likely that the intense training may contribute to a better streamlining shape. A correlation between the glide coefficient and the weekly training volume supported this notion, as these variables were positively correlated for both groups ($r = .810$ and $r = .779$ for the female and male groups respectively, $p < .001$). The findings of this study are in line with the findings of Chatard et al. (1990), who reported that swimmers with lower drag force had better swimming performance, which was assumed to be related to their higher gliding ability. In addition to the fact that a higher training volume equates to more streamlining practice and, presumably, better streamlining technique and performance, an increase in training volume may also contribute to the development of a more hydrodynamically favorable body morphology (trunk muscle hypertrophy) that may potentially lead to a broader chest and narrower waist. This could be explored further in future studies, to examine the links between training volume and potential changes in body morphology.

As the relative position of maximum cross-section to the whole length of a body for aquatic animals determines the point where the boundary layer separation is expected to occur, an increase in the relative position (i.e., shifting the maximum cross-sectional area further backward toward the trailing edge) is associated with a decrease in passive drag (Mordvinov, 1972). With no significant correlations between the relative position of the maximum cross-sectional area and the glide coefficient in the current study, this assumption might not be applicable to human bodies. This could be because of the differences between shape characteristics of a human and the more streamlined shapes of aquatic animals. It is possible that the irregular shape of the human body affects the flow condition in such way that the separation point cannot be predicted by the location of the maximum cross-sectional area (Clarys, 1979). As indicated in the rationale, the location of maximum cross-sectional area is an indicator of where the flow is likely to become separated from the body and it does not provide a certain location of flow separation, for which a flow visualization technique would be needed.

Fineness ratio of the upper body in this study was negatively correlated with the glide coefficient for the male group. The upper-body fineness ratio for the male group (4.99 ± 0.96) was higher than the optimal fineness ratio of 4.5 (Hertel, 1966). In this range, the drag coefficient was expected to increase with increasing fineness ratio. This could perhaps explain the negative correlation between the upper body fineness ratio and the glide coefficient.

Contrary to the results of Clarys (1978), who found a negative correlation between passive drag and fineness ratio, no correlation was found between the fineness ratio of the whole body and the glide coefficient in the current study. This discrepancy could be due to Clarys (1978) testing swimmers on the water surface and using the values of body height instead of streamlined height to calculate the fineness ratios. In such conditions, wave drag may cause other parameters to become important and the results may differ to those of submerged bodies. To minimize drag in general, a fuselage should be designed to minimize the exposed skin area or wetted surface, which generally implies the fuselage should be somewhat "egg shaped," with a fineness ratio of about 4.5. Limb internalization in the aquatic mammals and the presence of a tapered shape help them to follow this general rule in comparison with humans. However, a human body shape, which, in addition to not having a circular cross-sectional area, has humps, bumps and hollows that create local areas of pressure gradient. This makes the human body shape inferior to the well-streamlined shape of the aquatic mammals that have evolved with drag-reducing shape characteristics (Aleyev, 1977). Comparison of the glide coefficient of 15 at Reynolds number of 2.5 million for the sea lions (Feldkamp, 1987) with the average glide coefficient of 3.5 for the subjects participating in the current study emphasizes the scale of differences in gliding ability as a result of shape differences.

The positive (although nonsignificant) correlation between the waist to hip taper index may be due to a narrower range in this group (i.e., *SD* of 0.02 for male group as compared with *SD* of 0.04 for the female group). As can be seen in the corresponding table, the average values are –0.13 for both groups. This causes a higher coefficient of variation for the female (31%) than the male group (15%).

The chest to waist taper indices for both groups were positively correlated with the glide coefficient. This can perhaps be explained by the fact that the taper indices were negatively correlated with the drag coefficient according to a general trend in fluid dynamics (the higher the taper index, the higher the drag coefficient). As these indices determine the gradient of changes in two consecutive cross-sectional areas of the body, it seems that bodies with greater changes in cross-sectional areas from chest to waist have a lower drag coefficient that would help them to glide more efficiently. In the female group, a more acute change in cross-sectional area

between the waist and hip was correlated significantly with glide efficiency, indicating that the greater change in the cross-section between the waist and hip probably prevents flow being separated from the body. However, it should be emphasized that a very abrupt change in the cross-sectional area could result in sudden changes in the flow traveling over the body contours and in creating areas of flow separation (see Naemi et al., 2010).

Male swimmers with a higher ratio of chest to hip cross-sectional area showed a better streamlining characteristic by having a significantly higher glide coefficient. This could be explained by assuming that during glides the lower zone "drafts" the upper zone. As the chest and hip cross-sectional areas represent the maximum cross-sectional areas of the upper and the lower zones of the body, the lower the ratio of the maximum cross-sectional area of the drafting zone to the maximum cross-sectional area of the leading zone, the more the drafting zone would be able to take advantage of drafting and reduce resistive force. This may decrease the drag coefficient and consequently increase the glide coefficient, which could explain the positive correlation between the ratio of chest to hip cross-sectional area and the glide coefficient.

Male subjects with hyperextension in their hips and knees had lower glide coefficients, and hence glide efficiency, than male subjects with no hyperextension in these joints. It can be argued that the hyperextension of the hips causes the thigh and trunk to not be aligned, so that the water flows around the body with more disturbances than when the hips are extended. Hyperextension of knee and hip together may have resulted in separation of flow and an increase in the drag coefficient and, therefore, a decrease in the glide coefficient.

The results of this study have practical applications in talent identification with the aim of selecting novice swimmers with a potential of performing at a high level. The findings indicate that in talent identification the evaluation could prioritize the shape characteristics of the body. For example, swimmers who possess a higher chest to waist taper index are more likely to be able to glide more efficiently compared with the swimmers with a lower chest to waist taper index. Although the relative importance of different morphological indices may vary among swimmers, the results of the current study can be used as baseline data for talent identification and suggest that the emphasis should remain on the body shape characteristics. Nevertheless, as the shape of the body may change over the period of growth and maturation, a longitudinal study conducted over a number of years would be useful in developing a predictive model that would take into account the effect of such changes in the swimmer's body shape indices. As explained comprehensively in the hydro-kinematic method (Naemi and Sanders, 2008), to make sure that the joint segments and posture stay consistent over the course of a glide interval, the swimmers were asked to push with a moderate push-off and to maintain the gliding depth. This was the main reason for the gliding velocities in the current study being lower compared with the glides after push-off during competition (which might reach average velocities around 2 m/s). It should be emphasized that at higher speeds (e.g., 3 m/s), as the swimmer is closer to the surface the wave drag can also become influential (Naemi et al., 2010). In this case other morphological indices may become more important that may need further consideration with regards to talent identification.

The results of the correlation of certain joint angles with the hydrodynamic and glide efficiency parameters are helpful in developing an optimized streamlined posture with the aim of enhancing glide efficiency and, hence, swimming performance. In developing such a streamlined posture, specific attention needs to be paid to avoid hyperextension at the hip and knee joint angles, as this seems to decrease glide efficiency for male swimmers. Further studies must be conducted to explore in more details the effects of these angles and their optimal values for swimmers.

The findings of the current study could also have important applications in designing swimming suits for improving performance. Based on the positive correlation between gliding efficiency and the hip to waist taper index, it is possible that designing a swimming suit that compresses the waist area to further decrease its cross-sectional area (with a consequent increase in the taper index) may help to improve performance. Further studies are required to determine the optimal range of taper index for each individual, and to determine the tension characteristics of the suit for designing swimmer-specific suits. Obviously, such a swimming suit needs to comply with the relevant regulations so that it can be used in competitions.

In conclusion, this study showed that the glide efficiency of swimmers seems to increase when velocity decreases. Swimmers with superior shape characteristics were able to glide more efficiently than subjects who had large body mass with low cross-sectional area. Moreover, swimmers with superior shapes encountered lower resistance and were able to entrain more added mass of water than those with higher maximum cross-sectional area or higher body volume respectively. Thus, the difference of glide efficiency parameters between two bodies depends predominantly on the differences in shape characteristics, such as morphological indices and postural angles. Some of the morphological indices and joint angles investigated in this study were shown to affect glide efficiency. To further improve glide efficiency and swimming performance, future research should focus on identifying the optimal values of such indices and angles for different swimmers.

References

Aleyev, Y.G. (1977). *Nekton.* The Hague: Dr W. Junk b. v. Publishers.

Benjanuvatra, N., Blanksby, B.A., & Elliott, B.C. (2001). Morphology and hydrodynamic resistance in young swimmers. *Pediatric Exercise Science, 13*(3), 246–255.

Bixler, B., Pease, D., & Fairhurst, F. (2007). The accuracy of computational fluid dynamics analysis of the passive drag

of a male swimmer. *Sports Biomechanics, 6*(1), 81–98. PubMed doi:10.1080/14763140601058581

Chatard, J.C., Lavoie, J.M., Bourgoin, B., & Lacour, J.R. (1990). The contribution of passive drag as a determinant of swimming performance. *International Journal of Sports Medicine, 11*(5), 367–372. PubMed doi:10.1055/s-2007-1024820

Clarys, J.P. (1978). Relationship of human body form to passive and active hydrodynamic drag. In E. Asmussen & K. Jorgenson (Eds.), *Biomechanics VI-B* (pp. 120–125). Baltimore: University Park Press.

Clarys, J.P. (1979). Human morphology and hydrodynamics. In J. Terauds & E.W. Bedingfield (Eds.), *Swimming III* (pp. 3–41). Baltimore: University Park Press.

Clarys, J.P., Jiskoot, J., Rijken, H., & Brouwer, P.J. (1974). Total resistance in water and its relation to body form. In R.C. Nelson & C.A. Morehouse (Eds.), *Biomechanics IV* (pp. 187–196). Baltimore: University Park Press.

D'Acquisto, L.J., Costill, D.L., Gehlsen, G.M., Young, W.T., & Lee, G. (1988). Breaststroke economy skill and performance: study of breaststroke mechanics using a computer based "velocity video." *Journal of Swimming Research., 4,* 9–14.

Feldkamp, S.D. (1987). Swimming in the California sea lion: Morphometrics, drag and energetics. *The Journal of Experimental Biology, 131,* 117–135. PubMed

Fish, F.E., & Hui, C.A. (1991). Dolphin swimming: A review. *Mammal Review, B* (21), 181–195.

Hay, J.G., & Guimaraes, A.C.S. (1983). A quantitative look at the swimming biomechanics. *Swimming Technique, 20*(2), 11–17.

Hertel, H. (1966). *Structure-Form-Movement*. New York: Reinhold Publishing Corporation.

Jensen, R.K. (1978). Estimation of the biomechanical properties of three body types using a photogrammetric method. *Journal of Biomechanics, 11*(8-9), 349–358. PubMed doi:10.1016/0021-9290(78)90069-6

Lyttle, A.D., Blanksby, B.A., Elliott, B.C., & Lloyd, D.G. (1998). The effect of depth and velocity on drag during the streamlined glide. *Journal of Swimming Research, 13,* 15–22.

Miyashita, M., & Tsunoda, R. (1978). Water resistance in relation to body size. In B. Eriksson & B. Furberg (Eds.), *Swimming Medicine IV* (pp. 395–401). Baltimore: University Park Press.

Mordvinov, Y.E. (1972). Some hydrodynamic parameters of body shape in pinnipeds. *Hydrobiologia, 8,* 81–84.

Naemi, R., & Sanders, R.H. (2008). A "hydro-kinematic" method of measuring glide efficiency of a human swimmer. *Journal of Biomedical Engineering, 130*(6), 061016. doi:10.1115/1.3002764

Naemi, R., Easson, W.J., & Sanders, R.H. (2010). Hydrodynamic glide efficiency in swimming. *Journal of Science and Medicine in Sport, 13*(4), 444–448. PubMed doi:10.1016/j.jsams.2009.04.009

Wicke, J., & Lopers, B. (2003). Validation of the volume function within Jensen's (1978) elliptical cylinder model. *Journal of Applied Biomechanics, 19*(1), 3–12.